

Fluctuation suppression in microgels by polymer electrolytes

S. Pasini,^{1, a)} S. Maccarrone,¹ N. Szekely,¹ L. Stingaciu,² A. Gelissen,³ W. Richtering,⁴ M. Monkenbusch,⁵ and O. Holderer¹

¹⁾Forschungszentrum Jülich GmbH, JCNS at Heinz Maier-Leibnitz Zentrum, Lichtenbergstraße 1, 85747 Garching, Germany

²⁾NScD, Oak Ridge National Laboratory, Oak Ridge, TN 37831, USA

³⁾Institute of Physical Chemistry, RWTH Aachen University, 52056 Aachen, Germany

⁴⁾Institute of Physical Chemistry, RWTH Aachen University, 52056 Aachen and JARA-SOFT 52056 Aachen, Germany

⁵⁾Jülich Centre for Neutron Science (JCNS) & Institute for Complex Systems (ICS), Forschungszentrum Jülich GmbH, 52428 Jülich, Germany

(Dated: 5 May 2020)

Structural details of thermoresponsive, cationically poly(N-iso-propylacrylamide-co-methacrylamido propyl trimethyl ammonium chloride) P(NIPAM-co-MAPTAC) microgels and the influence of the anionic electrolyte polystyrene sulfonate (PSS) on the internal structure and dynamics of the cationic microgels has been studied with a combination of small angle neutron scattering (SANS) and neutron spin echo (NSE) spectroscopy. While SANS can yield information on the overall size of the particles and on the typical correlation length inside the particles, studying the segmental polymer dynamics with NSE gives access to more internal details which only appear due to their effect on the polymer motion. The segmental dynamics of the microgels studied in this paper is to a large extent suppressed by the PSS additive. Possible scenarios of the influence of the polyanions on the microgel structure and dynamics are discussed.

I. INTRODUCTION

Microgels are made of chemically cross-linked polymer chains, the typical size of the microgel is of the order of 100-1000 nm^{1,2}. A widely studied class of microgels are thermoresponsive, i.e. the solvent properties change from good to bad solvent when the temperature rises above the volume phase transition temperature (VPTT). Such microgels possess a large potential for application in, for example, drug delivery systems, responsive switches and functional coatings³. Neutron scattering has been used to investigate the structure of microgels with small angle neutron scattering (SANS), where the density profile of microgels with a dense core and a shell with decreasing polymer density has been determined. Also insight into the internal structure of microgels with complex architecture, e.g. core-shell microgels or hollow microgels has been obtained from SANS^{4,5}. Internal density fluctuations and inhomogeneities in microgels fabricated with batch and continuous monomer feeding approaches have been studied recently^{6,7}. The interaction of microgels with electrolytes has been studied with core-shell microgels with a cationic core and an anionic shell, where the uptake and release of polyelectrolytes could be controlled⁸. Microgels deposited on surfaces as a functional coating have been studied with microscopic techniques⁹⁻¹¹ and SANS under grazing incidence conditions (GISANS)^{12,13}, where deformations of internal heterogeneities can be observed. The dynamics of microgels has been accessed with neutron spin echo (NSE) spectroscopy^{6,7,14-19}. Structural inhomogeneities are often not fully accessible in such systems due to the intrinsic radial averaging of SANS. Still the fluctuations measured at different length scales by NSE have the potential of revealing details

of the microgel structure. A rather recent topic is the measurement of polymer chain dynamics at the solid-liquid interface with grazing incidence neutron spin echo spectroscopy (GINSES), the dynamic extension to GISANS. Microgel dynamics at the interface has been studied in references^{20,21}.

An interesting aspect is how the interaction of microgels with the ions can modify the dynamics of the gel. Previous works¹⁸ have shown that the addition of counterions, like for examples hexacyanoferrate, can slow down the internal dynamics of PNIPAM-co-MAPTAC-based microgels. This is likely due to the interaction between the ions and the unbalanced charges of the gel that tend to reduce the polymer length in a sort of pinning effect. Thus the segmental dynamics of the crossed-linked polymer is reduced. Starting from these results we would like to investigate how polyanions can affect the internal dynamics of PNIPAM-co-MAPTAC in the swollen state. As a method neutron spin echo provides the best observation window to reveal such dynamical effects.

II. EXPERIMENTAL

A. Sample Preparation

The microgels used in this study have been synthesized by precipitation polymerization. The amine group of the microgel was quaternized by 80% and is therefore permanently positively charged. Details of the synthesis are described elsewhere²² (see also the supporting information). Polystyrene sulfonate (PSS) with a low molecular weight (3780 g/mol), corresponding to about 20 monomer units, has been used as a polymer electrolyte additive. Deuterated PSS and protonated PSS have been used in order to vary the contrast conditions in the neutron scattering experiments. The cationic poly(N-iso-propylacrylamide-co-methacrylamido propyl trimethyl ammonium chloride)

^{a)}Corresponding author: s.pasini@fz-juelich.de

P(NIPAM-co-MAPTAC) microgels used here were synthesized as described in Ref.²². The microgels were dissolved in 0.1 M NaCl/D₂O in order to minimize incoherent scattering in the neutron scattering experiments.

B. Scattering Experiments

Small-angle neutron scattering (SANS) experiments were carried out on KWS-2^{23,24}, operated by the Jülich Centre for Neutron Science (JCNS) at the research reactor FRM II of the Heinz Maier-Leibnitz Zentrum (MLZ) in Garching, Germany. To probe a wide Q -range (from circa 0.002 up to 0.2 Å⁻¹) measurements were performed at sample-to-detector distances of 8 and 30 m on KWS-2 at a wavelength of 5 Å. The following samples were measured at 20° C, which is below the VPTT of the microgel: PNIPAM-co-MAPTAC amine microgel (0.6% wt) alone and with addition of either deuterated or protonated polystyrene sulfonate (dPSS, hPSS, 0.1% wt). The concentration of the microgel remained the same also after addition of PSS, for the SANS measurement. As a solvent D₂O has been used in order to achieve the best microgel-environment contrast. Salt (NaCl) and HCl were also added. The final pH of the solution was 3. For intensity calibration empty cell and plexiglass were also measured. Data treatment was performed with QtiKWS10 software.

For the NSE experiments, the measurements have been performed at the SNS-NSE instrument (BL-15) at the spallation neutron source (SNS, Oak Ridge, TN, USA)²⁵. Consistently with the SANS experiment, also with NSE we measured the PNIPAM-co-MAPTAC amine microgel alone and with addition of either hPSS or dPSS. As background sample we measured the solvent D₂O and NaCl (with HCl, pH=3) with and without PSS. The mass concentration of the samples were either 1.2% or 0.6% of PNIPAM-co-MAPTAC, the former without PSS, the latter with 0.1% of PSS. Concentrations higher than about 1% wt are desirable for the NSE experiments to have a coherent scattering signal well above the incoherent level. Nonetheless we had to reduce the concentration of polymer in the NSE experiment when we added the PSS in order to avoid the formation of precipitate in the cell. All the measurements have been performed with Hellma 1mm quartz cells, at a temperature of 20° C and at different values of the momentum transfer Q . The data have been reduced by means of the new program for NSE-data reduction DrSpine²⁶.

III. EXPERIMENTAL RESULTS

A. Structural analysis

An experiment with small angle neutron scattering is essential to understand whether the addition of the polyanions has caused any structural modification of the microgel. The SANS data for the PNIPAM-co-MAPTAC with and without PSS are shown in figure 1. In the region of Q of interest for the NSE the scattered intensity of the PNIPAM-co-MAPTAC

presents the expected Q^{-2} power law behaviour. For smaller values of the scattering vector, a small elongation of the curve between the Q^{-2} and the Q^{-6} regime can be observed for the samples with PSS.

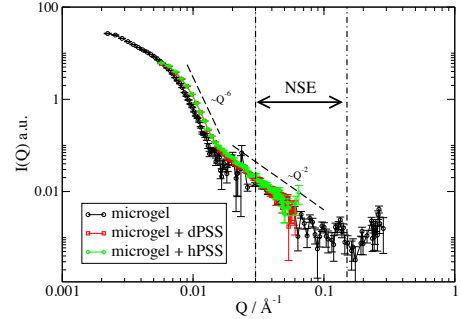


FIG. 1. All SANS data for PNIPAM-co-MAPTAC at 20° C with and without PSS with background subtracted. The region between the dot-dashed lines marks the Q accessible by the NSE technique.

We use a model that combines the “fuzzy-sphere” model, for the small Q regime, with an Ornstein-Zernike term for larger Q ¹⁶. The fuzzy-sphere model

$$I_S(Q) = A \int_0^\infty P(Q, R)^2 e^{-(\sigma_{surf} Q)^2} G(R, \langle R \rangle, \sigma_{pol}) dR, \quad (1)$$

consists of the form factor of a sphere $P(Q, R) = 3(\sin(QR) - QR \cos(QR))^2 / (QR)^3$ convoluted with the Gaussian

$$G(R, \langle R \rangle, \sigma_{pol}) = \frac{\exp \left[-\frac{(R - \langle R \rangle)^2}{2\sigma_{pol}^2} \right]}{\sqrt{2\pi\sigma_{pol}^2}} \quad (2)$$

to account for the polydispersity of the microgel. σ_{surf} is different from zero for a non-homogeneous cross-linking density. The amplitude A is proportional to the number density of the microgel particles, to the volume of the polymer in a particle and to the contrast between the scattering length of the polymer and the solvent. The Ornstein-Zernike term is given by

$$I_{therm} = \frac{I_{OZ}}{1 + \xi^2 Q^2}, \quad (3)$$

where ξ is the correlation length of the thermal fluctuations. The complete scattering intensity is then

$$I(Q) = I_{therm}(Q) + I_S(Q). \quad (4)$$

Equation 4 is a standard model for PNIPAM-co-MAPTAC in the swollen state.

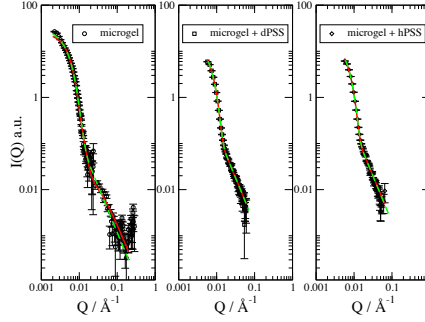


FIG. 2. SANS data for the microgel without and with PSS with background subtracted and fitted with Eq. 4 (solid red) compared to the fit where the Ornstein-Zernike function is approximated as in Eq. 5 (dashed green) lines.

Figures 2 show the SANS data for the microgel with and without the PSS fitted according to 4.

When one applies the Ornstein-Zernike model one has to keep in mind that ξ and I_{OZ} are correlated if the analysis relies on data with ξQ much larger than 1. So the question is whether it is correct to fit them independently. However, when $(\xi Q)^2 > 1$ Eq. 3 can be approximated as

$$I_{therm} \simeq \frac{1}{(\Xi Q)^2}, \quad (5)$$

where Ξ is defined as $\xi/\sqrt{I_{OZ}}$. The dashed lines in figures 2 show that a simple Q^{-2} power law can describe very well the SANS data at larger Q . The extracted values for $\frac{1}{\Xi^2}$ are reported in table I.

TABLE I. The values for R_{box} , R_{SANS} as well as for the rescaled correlation length ($\Xi^{-2} = I_{OZ}/\xi^2$) obtained from the model $I(Q) = I_{therm}(Q) + I_S(Q)$ where $I_{therm}(Q)$ is given by Eq. 5. The digits in brackets for the calculated values of the last column represent the standard uncertainty. The units for Ξ are \AA divided by the units of the intensity (cm^{-1}).

	R_{box} [\AA]	R_{SANS} [\AA]	$1/\Xi^2$	$\xi/\sqrt{I_{OZ}}$
microgel	385 ± 2	797 ± 4	$(11.8 \pm 0.1) \times 10^{-6}$	29(1)
microgel + dPSS	220 ± 10	660 ± 20	$(17.8 \pm 0.1) \times 10^{-6}$	27(3)
microgel + hPSS	230 ± 10	680 ± 20	$(20.0 \pm 0.1) \times 10^{-6}$	22(3)

The density of cross linking of the microgel is higher in the core and is characterised by a box profile up to a radius given by $R_{box} = \langle R \rangle - 2\sigma_{surf}$ ^{16,27}. The parameter σ_{surf} describes the decreasing of the cross-linking density near the surface of the microgel. At the radius $\langle R \rangle$ the profile has decreased to half of the core density while it is already close to zero

at $R_{SANS} = \langle R \rangle + 2\sigma_{surf}$, which is the overall size of the microgel as given by SANS.

B. Dynamics

For temperatures smaller than the transition temperature VPTT the microgel is in the so-called swollen state. The main focus of this paper is to study the effect of polyanions on the dynamics of the microgel in this state. For this purpose we carried out an experiment with the neutron spin echo (NSE) which provides the highest resolution among neutron spectrometers.

Thanks to the property of the new program for data-reduction DrSpine, that allows for a custom binning, up to 20 Q bins could be extracted from the experimental data. For sake of clarity, in figure 3 only some selected curves for the normalized intermediate scattering function ($S(Q,t)/S(Q,0)$) are shown. The curves are already background corrected, as a background we considered D_2O with NaCl. In order to control whether contributions from the internal dynamics of the polystyrene sulfonate are present and to what degree these can affect our analysis, a second salt solution containing hPSS (at the same concentration as the one used in the samples with the microgel) was also measured. We could assert that the dynamical content of the PSS at the considered concentration is not relevant and it is indeed comparable with that of the background, i.e. D_2O with NaCl.

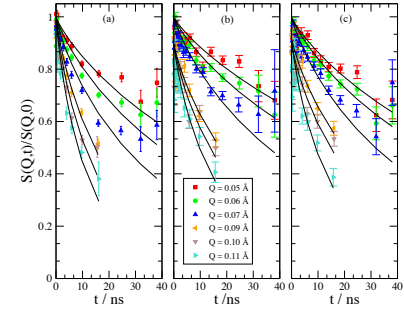


FIG. 3. NSE data after background subtraction: (a) PNIPAM-co-MAPTAC, (b) PNIPAM-co-MAPTAC with dPSS and (c) PNIPAM-co-MAPTAC with hPSS. The fit has been performed with Eq. 6. For sake of clarity only some selected curves are shown.

It is widely observed^{6,7,14-18} that NSE data for microgels can be fitted well with a stretched exponential function

$$\frac{S(Q,t)}{S(Q,0)} = I_0 \exp \left[- \left(\frac{t}{\tau_0} \right)^\beta \right], \quad (6)$$

where typically $\beta = 0.85$ for Zimm dynamics²⁸ and I_0 is the intercept at $t \rightarrow 0$.

The experimental curves seem to suggest that the PSS tends to slow down the dynamics of the polymer. For a better understanding of the problem we extract the effective diffusion coefficient from Eq. 6 according to

$$D_{eff} = \frac{\beta}{\tau_0 \Gamma(\beta^{-1}) Q^2}. \quad (7)$$

The extracted values for D_{eff} are shown in figure 4 for the PNIPAM-co-MAPTAC with and without PSS.

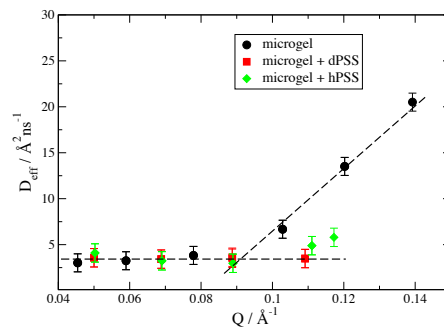


FIG. 4. Effective diffusion coefficients as from Eq. 7 with $\beta = 0.85$

The same behaviour for D_{eff} is obtained if the NSE data are fitted with Eq. 6 and $\beta = 1$.

Equation 6 is used here as a rather generic function for the decay of the intermediate scattering function. It describes the pure segmental chain dynamics with $\beta = 0.85$ but also a mixture of diffusion and segmental dynamics would result in a slightly modified stretching exponent. Here we focus on the relaxation time τ_0 as a function of Q . The value of β does not play a crucial role in the data evaluation, and cannot be determined better with the given Fourier time range. The contribution of the diffusion of the overall particle, $S(Q, t)/(S(Q, 0)) = \exp(-DQ^2 t)$ with the Stokes-Einstein diffusion Coefficient $D = k_B T / (6\pi\eta R_h)$ and the hydrodynamic radius (R_h) of 80 nm from DLS (see the supplementary material) is rather low. This is implicitly included in the Q -dependence of the relaxation rate, which is in the beginning dominated not by the overall diffusion, but by the density fluctuations on shorter length scales within the microgel particle, which also have a diffusive character.

IV. DISCUSSION

The SANS data for all the samples can be described quite well by a combination of fuzzy-sphere and Ornstein-Zernike

model. The results of the analysis is a contraction of the average radius suggesting a sort of collapse of the microgel due to the presence of PSS in solution^{29,30}. The SANS data at larger Q can be well fitted by a single-parameter model consisting of a Q^{-2} power-law. The values obtained for Ξ reported in table I provide an estimate of the correlation length if one assumes that the intensity does not change much between the samples. We find that Ξ remains almost unchanged or they rather decrease in the presence of PSS (see), which is consistent with the hypothesis that the microgel shrinks.

The picture delivered by the SANS data is thus a shrunken microgel upon PSS addition. The almost unchanged intensity upon hPSS addition compared to dPSS addition might indicate that it is not uniformly penetrating the whole microgel. We would have expected a higher contrast in the former case if the protonated polyanions fully goes into the full volume of the microgel. A more quantitative SANS analysis could shed light onto this question and is left for future investigations.

Internal fluctuations of microgels have been studied with neutron spin echo spectroscopy. The addition of PSS had a strong influence on the local dynamics of the cationic microgel segmental motion and density fluctuations.

The typical transition from diffusive dynamics of density fluctuations to Zimm dynamics of individual segments, which takes place typically at length scales of the microgel mesh size, is suppressed and diffusive fluctuations strongly dominate upon addition of PSS. To our knowledge this is a new result. The PSS used in this study has a length of approximately 20 monomer units. Polyanions can replace the monovalent counterions inside the microgel, which has been reported e.g. in Ref³¹ for gels. The loss of monovalent counterions could reduce the osmotic pressure inside the microgel, resulting in a shrinking of it.

The decrease of the correlation length is in agreement with the disappearing of the internal fluctuations in the samples with PSS. Indeed if the complexation of the microgel by the PSS reduces the correlation length then the Zimm dynamics is to be expected at smaller length scales and therefore the transition from the Q^2 to the Q^3 behavior in the NSE should occur at larger Q .

The collapse of the microgel by the PSS addition impedes, or partially suppresses, some of the internal modes of the polymer (figure 5). This way of interacting with counterions appears different with respect to that observed in¹⁸ between PNIPAM and hexacyanoferrate. The absorbed ions created additional "charge" cross-linkers, acting as an apparent secondary network that slowed down the dynamics of the microgel. But an evident suppression of internal modes was not observed in the case of the relatively small hexacyanoferrate molecules in Ref.¹⁸. The PSS on the other hand seems to suppress Zimm dynamics on the observed length- and time-scales, which might come from the complexation of the polyanions with the cationic microgel.

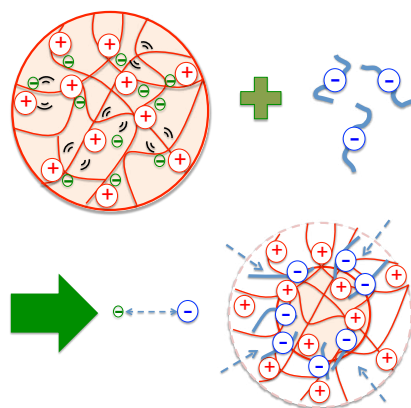


FIG. 5. Possible representation of the interaction between the microgel and the PSS: the negative charges in green stand for the monovalent counterions while the bigger charges in blue represent the PSS polyanions.

V. CONCLUSIONS

In the present study we investigate the suppression of the internal dynamics of PNIPAM-co-MAPTAC microgel in presence of anionic polyelectrolyte polystyrene sulfonate. A combination of small angle neutron scattering and neutron spin echo showed that the microgel, originally in the swollen state, goes through a transition into a sort of collapsed state due to the presence of the PSS. In this state some of the motions between the cross links are suppressed, at least in the region of Q accessible with the NSE technique, and diffusive fluctuations strongly dominate.

SUPPLEMENTARY MATERIAL

The supplementary material includes details on the synthesis of the microgel and its chemical characterisation as well as on the dynamic light scattering (DLS) measurement performed on the sample.

ACKNOWLEDGEMENTS

This research work was supported by the Deutsche Forschungsgemeinschaft within the Sonderforschungsbereich (SFB 985), "Functional Microgels and Microgel Systems". Data available on request from the authors.

¹R. Pelton, "Temperature-sensitive aqueous microgels," *Advances in colloid and interface science* **85**, 1–33 (2000).

²A. Pich and W. Richtering, *Chemical design of responsive microgels*, Vol. 234 (Springer, 2010).

³M. Karg, A. Pich, T. Hellweg, T. Hoare, L. A. Lyon, J. J. Crassous, D. Suzuki, S. Gumerov, R. A. and Schneider, I. I. Potemkin, and W. Richtering, "Nanogels and microgels: From model colloids to applications, recent developments, and future trends," *Langmuir* **35**, 6231–6255 (2019).

⁴J. Dubbert, T. Honold, J. S. Pedersen, A. Radulescu, M. Drechsler, M. Karg, and W. Richtering, "How hollow are thermoresponsive hollow nanogels?" *Macromolecules* **47**, 8700–8708 (2014).

⁵A. C. Nickel, A. Scotti, J. E. Houston, T. Ito, J. Crassous, J. S. Pedersen, and W. Richtering, "Anisotropic hollow microgels that can adapt their size, shape, and softness," *Nano letters* **19**, 8161–8170 (2019).

⁶T. Kyrey, J. Witte, A. Feoktystov, V. Pipich, B. Wu, S. Pasini, A. Radulescu, M. U. Witt, M. Kruteva, R. von Klitzing, *et al.*, "Inner structure and dynamics of microgels with low and medium crosslinker content prepared via surfactant-free precipitation polymerization and continuous monomer feeding approach," *Soft matter* **15**, 6536–6546 (2019).

⁷J. Witte, T. Kyrey, J. Lutzki, A. M. Dahl, J. Houston, A. Radulescu, V. Pipich, L. Stingaciu, M. Kühnhammer, M. U. Witt, *et al.*, "A comparison of the network structure and inner dynamics of homogeneously and heterogeneously crosslinked pnipam microgels with high crosslinker content," *Soft matter* **15**, 1053–1064 (2019).

⁸A. P. Gelissen, A. Scotti, S. K. Turnhoff, C. Janssen, A. Radulescu, A. Pich, A. A. Rudov, I. I. Potemkin, and W. Richtering, "An anionic shell shields a cationic core allowing for uptake and release of polyelectrolytes within core-shell responsive microgels," *Soft Matter* **14**, 4287–4299 (2018).

⁹M. U. Witt, S. Hinrichs, N. Möller, S. Backes, B. Fischer, and R. von Klitzing, "Distribution of coFe2o4 nanoparticles inside pnipam-based microgels of different cross-linker distributions," *The Journal of Physical Chemistry B* **123**, 2405–2413 (2019).

¹⁰M. F. Schulte, A. Scotti, A. P. Gelissen, W. Richtering, and A. Mourran, "Probing the internal heterogeneity of responsive microgels adsorbed to an interface by a sharp sfn tip: Comparing core-shell and hollow microgels," *Langmuir* **34**, 4150–4158 (2018).

¹¹E. Siemes, O. Nevskiy, D. Sysoiev, S. K. Turnhoff, A. Oppermann, T. Huhn, and D. Richtering, "Nanoscope visualization of cross-linking density in polymer networks with diarylethene photoswitches," *Angew. Chem. Int. Ed. Engl.* **57**, 12280–12284 (2018).

¹²T. Kyrey, M. Kaneva, K. Gawlitza, J. Witte, R. von Klitzing, O. Soltwedel, Z. Di, S. Wellert, and O. Holderer, "Grazing incidence x-ray and reflectometry combined with simulation of adsorbed microgel particles," *Physica B: Condensed Matter* **551**, 172–178 (2018).

¹³T. Kyrey, J. Witte, V. Pipich, A. Feoktystov, A. Koutsoubas, E. Vezhlev, H. Frielinghaus, R. von Klitzing, S. Wellert, and O. Holderer, "Influence of the cross-linker content on adsorbed functionalized microgel coatings," *Polymer* **169**, 29–35 (2019).

¹⁴T. Hellweg, K. Kratz, S. Pouget, and W. Eimer, "Internal dynamics in colloidal pnipam microgel particles immobilised in mesoscopic crystals," *Colloids and Surfaces A: Physicochemical and Engineering Aspects* **202**, 223–232 (2002).

¹⁵M. Karg, S. Prevost, A. Brandt, D. Wallacher, R. von Klitzing, and T. Hellweg, "Poly-nipam microgels with different cross-linker densities," in *Intelligent Hydrogels* (Springer, 2013) pp. 63–76.

¹⁶S. Maccarrone, C. Scherzinger, O. Holderer, P. Lindner, M. Sharp, W. Richtering, and D. Richter, "Conosolvency effects on the structure and dynamics of microgels," *Macromolecules* **47**, 5982–5988 (2014).

¹⁷S. Maccarrone, A. Ghavami, O. Holderer, C. Scherzinger, P. Lindner, W. Richtering, D. Richter, and R. G. Winkler, "Dynamic structure factor of core-shell microgels: A neutron scattering and mesoscale hydrodynamic simulation study," *Macromolecules* **49**, 3608–3618 (2016).

¹⁸S. Maccarrone, O. Mergel, F. A. Plamper, O. Holderer, and D. Richter, "Electrostatic effects on the internal dynamics of redox-sensitive microgel systems," *Macromolecules* **49**, 1911–1917 (2016).

¹⁹C. Scherzinger, O. Holderer, D. Richter, and W. Richtering, "Polymer dynamics in responsive microgels: Influence of cononsolvency and microgel architecture," *Phys Chem Chem Phys* **14**, 2762–2768 (2012).

²⁰K. Gawlitza, O. Ivanova, A. Radulescu, O. Holderer, R. von Klitzing, and S. Wellert, "Bulk phase and surface dynamics of peg microgel particles," *Macromolecules* **48**, 5807–5815 (2015).

²¹S. Wellert, J. Hübner, D. Boyaciyan, O. Ivanova, R. von Klitzing, O. Soltwedel, and O. Holderer, "A grazing incidence neutron spin echo study of near surface dynamics in p (meo 2 ma-co-ogma) copolymer

This is the author's peer reviewed, accepted manuscript. However, the online version of record will be different from this version once it has been copyedited and typeset.

PLEASE CITE THIS ARTICLE AS DOI: 10.1063/4.0000014

- brushes," *Colloid and Polymer Science* **296**, 2005–2014 (2018).
- ²²A. P. Gelissen, A. J. Schmid, F. A. Plamper, D. V. Pergushov, and R. Walter, "Quaternized microgels as soft templates for polyelectrolyte layer-by-layer assemblies," *Polymer* **55**, 1991–1999 (2014).
- ²³A. Radulescu, N. Kinga Szekely, and M.-S. Appavou, "Heinz maier-leibnitz zentrum et al. (2015). kws-2: Small angle scattering diffractometer," *Journal of large-scale research facilities* **1**, A29 (2015).
- ²⁴A. Radulescu, V. Pipich, H. Frielinghaus, and M.-S. Appavou, "Kws-2, the high intensity / wide q-range small- angle neutron diffractometer for soft-matter and biology at frn ii," *Journal of Physics: Conference Series* **351**, 012026 (2012).
- ²⁵M. Ohl, M. Monkenbusch, N. Arend, T. Kozielski, G. Vehres, C. Tie-mann, M. Butzek, H. Soltner, U. Giesen, R. Achten, H. Stelzer, B. Lind-nau, A. Budwig, H. Kleines, M. Drochner, P. Kaemmerling, M. Wa-gener, R. Moeller, E. B. Iverson, M. Sharp, and D. Richter, "The spin-echo spectrometer at the spallation neutron source (sns)," *Nuclear Instruments & Methods in Physics Research Section A-Accelerators Spectrometers De-tectors and Associated Equipment* **696**, 85–99 (2012).
- ²⁶P. A. Zolnierczuk, O. Holderer, S. Pasini, T. Kozielski, L. R. Stingaciu, and M. Monkenbusch, "Efficient data extraction from neutron time-of-flight spin-echo raw data," *Journal of Applied Crystallography* **52**, 1022–1034 (2019).
- ²⁷C. Scherzinger, P. Lindner, M. Keerl, and W. Richtering, "Cononsolvency of poly(n,n-diethylacrylamide) (pdeaam) and poly(n-isopropylacrylamide) (pnipam) based microgels in water/methanol mixtures: Copolymer vs core-shell microgel," *Macromolecules* **43**, 6829–6833 (2010).
- ²⁸D. Richter, M. Monkenbusch, A. Arbe, and J. Colmenero, "Neutron spin echo in polymer systems," *Adv Polym Sci* **174**, 1–221 (2005).
- ²⁹W. Wong, J. E. and Richtering, "Layer-by-layer assembly on stimuli-responsive microgels," *Current Opinion in Colloid and Interface Science* **13**, 403–412 (2008).
- ³⁰J. Kleinen and W. Klee, A. and Richtering, "Influence of architec-ture on the interaction of negatively charged multisensitive poly(n-isopropylacrylamide)-co-methacrylic acid microgels with oppositely charged polyelectrolyte: Absorption vs adsorption," *Langmuir* **26**, 11258–11265 (2010).
- ³¹V. A. Kabanov, A. B. Zevin, V. B. Rogacheva, and V. A. Prevish, "Active transport of linear polyions in oppositely charged swollen polyelectrolyte networks," *Makromol. Chem.* **190**, 2211–2216 (1989).